Synthesis of Mesostructured Titania with Controlled Crystalline Framework

Hongmei Luo, Cheng Wang, and Yushan Yan*

Department of Chemical and Environmental Engineering, University of California, Riverside, California 92521

Received March 12, 2003. Revised Manuscript Received May 27, 2003

A simple synthetic approach to generate thermally stable mesostructured titania with controlled crystalline framework is reported. Large-pore mesoporous titania with pure anatase, rutile, bicrystalline (anatase and rutile), and tricrystalline (anatase, rutile, and brookite) frameworks are successfully synthesized by block copolymer templating method through simply varying the solvent and cosolvent (methanol, ethanol, 1-butanol, or 1-octanol, with or without water). Acidity is believed to determine the crystal structure formation. The crystalline mesoporous titania are characterized by X-ray diffraction (XRD), thermogravimetric and differential thermal analysis (TG/DTA), scanning electron microscopy (SEM), transmission electron microscope (TEM), UV−vis absorption spectroscopy, and N_2 adsorption/desorption measurements.

1. Introduction

The discovery of the M41S family of ordered mesoporous silica by Mobil in 1992 opened up a new era in the synthesis of porous materials.[1] Among mesoporous transition metal oxides, titanium dioxide (titania) is attractive because of its excellent performance in photocatalytic reactions. It is known that the basic requirements for photoactive materials are high crystallinity and large surface area. Thus, high-surface-area mesoporous titania with controlled crystalline framework is an important material. Mesoporous titania has been synthesized by controlling the high reactivity of Ti(IV) with the addition of stabilizing agents, such as phosphate,[2−6] amine,[6−11] ionic,[12−14] block polymer,[15−20] or nonionic surfactants as templates,[21] or nonsurfactant templates.[22−26] Mesoporous amorphous titania was first reported in 1995 by using alkyl phosphate surfactant through a modified sol−gel process.[2] However, it was not pure titania, and phosphorus was bound strongly to the molecular sieve, thus affecting its catalyst properties.[2−5] The phosphorus-free amorphous pure mesoporous titania was synthesized by using dodecylamine surfactants in combination with a dry aging technique.[7] These materials had a high surface area of 700 m^2/g, but they were not thermally stable.[7] The thermally stable mesoporous titania with large pore diameter and semicrystalline anatase framework was synthesized by amphiphilic poly (alkylene oxide) block copolymer as structure-directing agent in a nonaqueous (ethanol) solution.[15]

Titania exists in three naturally occurring polymorphs: anatase, rutile, and brookite. Each structure exhibits different physical properties and has different applications. Under ambient conditions, macrocrystalline rutile is thermodynamically stable relative to macrocrystalline anatase and brookite. However, thermodynamic stability is particle-size dependent, and at particle diameters below ca. 14 nm, anatase is more stable than rutile.[27] This may explain why anatase can

* To whom correspondence should be addressed. E-mail: yushan.yan@ucr.edu.

(1) Kresge, C. T.; Leonowicz, M. E.; Roth, W. J.; Vartuli, J. C.; Breck, J. S. *Nature* **1992**, *359*, 710.
(2) Antonelli, D. M.; Ying, J. Y. *Angew. Chem., Int. Ed. Engl.* **1995**, *34*, 2014.
(3) Putnam, R. L.; Nakagawa, N.; McGrath, K. M.; Yao, N.; Aksay, I. A.; Gruner, S. M.; Navrotsky, A. *Chem. Mater.* **1997**, *9*, 2690.
(4) Stone, V. F., Jr.; Davis, R. J. *Chem. Mater.* **1998**, *10*, 1468.
(5) Fujii, H.; Ohtaki, M.; Eguchi, K. *J. Am. Chem. Soc.* **1998**, *120*, 6832.
(6) Dai, Q.; Shi, L. Y.; Luo, Y. G.; Blin, J. L.; Li, D. J.; Yuan, C. W.; Su, B. L. *J. Photochem. Photobiol., A: Chem.* **2002**, *148*, 295.
(7) Antonelli, D. M. *Microporous Mesoporous Mater.* **1999**, *30*, 315.
(8) Wang, Y.; Tang, X.; Yin, L.; Huang, W.; Hacohen, Y. R.; Gedanken, A. *Adv. Mater.* **2000**, *12*, 1183.
(9) Miyake, Y.; Kondo, T. *J. Chem. Eng. Japn.* **2001**, *34*, 319.
(10) Yoshitake, H.; Sugihara, T.; Tatsumi, T. *Chem. Mater.* **2002**, *14*, 1023.
(11) Wang, Y.-D.; Ma, C.-L.; Sun, X.-D.; Li, H.-D. *Mater. Lett.* **2002**, *54*, 359.
(12) On, D. T. *Langmuir* **1999**, *15*, 8561.
(13) Cabrera, S.; Haskouri, J. E.; B-Porter, A.; B-Porter, D.; Marcos, M. D.; Amorós, P. *Solid State Sci.* **2000**, *2*, 513.
(14) Soler-Illia, G. J. de A. A.; Louis, A.; Sanchez, C. *Chem. Mater.* **2002**, *14*, 750.
(15) Yang, P.; Zhao, D.; Margolese, D. I.; Chmelka, B. F.; Stucky, G. D. *Nature* **1998**, *396*, 152. Yang, P.; Zhao, D.; Margolese, D. I.; Chmelka, B. F.; Stucky, G. D. *Chem. Mater.* **1999**, *11*, 2813.
(16) Yue, Y.; Gao, Z. *Chem. Commun.* **2000**, 1755.
(17) Peng, Z.; Shi, Z.; Liu, M. *Chem. Commun.* **2000**, 2125.
(18) Yu, J. C.; Zhang, L.; Yu, J. *New J. Chem.* **2002**, *26*, 416. Yu, J. C.; Zhang, L.; Yu, J. *Chem. Mater.* **2002**, *14*, 4647.
(19) Alberius, P. C. A.; Frindell, K. L.; Hayward, R. C.; Kramer, E. J.; Stucky, G. D.; Chmelka, B. F. *Chem. Mater.* **2002**, *14*, 3284.
(20) Tian, B.; Yang, H.; Liu, X.; Xie, S.; Yu, C.; Fan, J.; Tu, B.; Zhao, D. *Chem. Commun.* **2002**, 1824.
(21) Kluson, P.; Kacer, P.; Cajthaml, T.; Kalaji, M. *J. Mater. Chem.* **2001**, *11*, 644.
(22) Saadoun, L.; Ayllón, J. A.; Jiménez-Becerril, J.; Peral, J.; Domènech, X.; Rodríguez-Clemente, R. *Appl. Catal. B* **1999**, *21*, 269
(23) Zheng, J.-Y.; Pang, J.-B.; Qiu, K.-Y.; Wei, Y. *J. Mater. Chem.* **2001**, *11*, 3367.
(24) Devi, G. S.; Hyodo, T.; Shimizu, Y.; Egashira, M. *Sensors Actuators B* **2002**, *87*, 122.
(25) Guo, C.-W.; Cao, Y.; Dai, W.-L.; Fan, K.-N.; Deng, J.-F. *Chem. Lett.* **2002**, 588.
(26) Zhang, Y.; Weidenkaff, A.; Reller, A. *Mater. Lett.* **2002**, 54, 375.

10.1021/cm0302882 CCC: $25.00
Published on Web 08/22/2003

be synthesized as ultrafine particles, and few results concerning the preparation of nano rutile with large surface area at low temperature have been available. Anatase has large band gap energy and suitable redox potentials for practical use in photocatalysis and photoelectronics. Rutile is used for its high dielectric constant and high electrical resistance in the electronics industry for applications such as capacitors, filters, power circuits, and temperature compensating condensers. Furthermore, it is widely accepted that the mixed phase of the same semiconductor is beneficial in reducing the recombination of photogenerated electrons and holes and in enhancing photocatalytic activity.[28−30] For example, the high activity of standard titania catalyst Degussa P-25 is partially due to its composite nature consisting of 80% anatase and 20% rutile with a BET surface area of 50 m^2/g.[22] Thus, it is important to develop synthetic methods in which the pore size and the crystalline phase of titania can be controlled.

Until recently, mesoporous titania with amorphous, semicrystalline anatase, crystalline anatase, or bicrystalline with anatase and brookite frameworks have been reported. As mentioned earlier, thermally stable mesoporous titania was prepared by block copolymer templating method. However, only ethanol was used as solvent and anatase was obtained. In this study, we use $TiCl_4$ as the inorganic Ti source and block copolymer as the structure-directing agent. By simply varying the solvent used among methanol, ethanol, 1-butanol, or 1-octanol, and with or without a cosolvent of deionized distilled (DD) water, we successfully prepared mesoporous titania with pure anatase, pure rutile, bicrystalline (anatase and rutile) with controlled phase composition, or tricrystalline (anatase, rutile, and brookite) frameworks. It is noted that mesoporous pure rutile and tricrystalline titania have not been prepared previously.

2. Experimental Section

2.1. Preparation. The block copolymer surfactants $EO_{106}PO_{70}EO_{106}$ (F-127, EO = $-CH_2CH_2O-$, PO = $-CH_2(CH_3)CHO-$) and $EO_{20}PO_{70}EO_{20}$ (Pluronic P-123) were gifts from BASF. $TiCl_4$ was used as a titanium source and purchased from Alfa Aesar, and methanol, ethanol, 1-butanol, and 1-octanol were from Aldrich. All chemicals were used as received.

Mesoporous titania was prepared as follows. First, 1 g of the triblock copolymer F-127 was dissolved in 10 g of methanol, ethanol, 1-butanol, or 1-octanol by stirring for 10 min. Then 0.005 mol of $TiCl_4$ was added with vigorous stirring for 10 min, followed by dropwise addition of 0 or 0.03 mol DD H_2O with further stirring for 10 min. Finally, the sol was gelled at 40 °C in air for 3−10 days. Unless otherwise specified, the gel samples were calcined at 380 °C for 5 h with a heating rate of 100 °C/h and cooling rate of 60 °C/h in air to remove the surfactant before characterization.

2.2. Characterization. The X-ray diffraction (XRD) patterns were obtained on a Siemens D-500 diffractometer using Cu Kα radiation. Scanning electron microscopy (SEM) images were obtained in a Philips XL30-FEG operated at 20 kV. Transmission electron microscopy (TEM) images and electron diffraction pattern were performed on a Philips CM300 equipped with energy-dispersive X-ray (EDX) spectrometer and operated at 300 kV. Thermogravimetric and differential thermal analyses (TG/DTA) was performed on a TA Instruments SDT 2960 simultaneous DSC-TGA instrument at a heating rate of 10 °C/min in flowing nitrogen gas to investigate the decomposition of the surfactant. Nitrogen adsorption−desorption measurements were carried out at 77 K on a Micromeritics ASAP 2010 instrument to determine the Brunauer−Emmett−Teller (BET) surface area, and to estimate the pore size distribution using Barrett−Joyner−Halenda (BJH) procedures. Before measurement, samples were evacuated overnight at 200 °C and 1 μTorr. The pore volume was taken from the desorption branch of the isotherm at $P_i/P_0 = 0.98$ assuming complete pore saturation. UV−vis absorbance spectra were taken on a Cary UV−visible spectrophotometer. The titania colloid suspensions for UV−vis measurements were prepared by ultrasonically dispersing the sample in ethanol.

Table 1. Synthetic Conditions for Mesoporous TiO_2[a]

sample	solvent	aging time (days)	phase content[b]	crystalline size[c] (nm)
Ti-M	methanol	3	pure A	12
Ti-MH	methanol+H_2O	3	A(75%) + R(25%)	12(A)
Ti-E	ethanol	6	A(80%) + R(20%)	16(A)
Ti-E (P-123)	ethanol	6	A(52%) + R(48%)	17(A)
Ti-EH	ethanol+H_2O	6	A(48%) + R(32%) + B(20%)	13(A)
Ti-HCl	ethanol+HCl	6	pure R	16
Ti-B	1-butanol	7	A(33%) + R(65%)	14(R)
Ti-BH	1-butanol+H_2O	7	pure R	14
Ti-OH	1-octanol+H_2O	10	pure R	20

[a] Mesoporous TiO_2 was prepared by copolymer templating method. The starting sol contained 0.005 mol $TiCl_4$, 1 g of surfactant F-127, 10 g of methanol, ethanol, 1-butanol, or 1-octanol, with or without 0.03 mol DD H_2O. For Ti-HCl sample, 2 mL of concd HCl was used. Surfactant P-123 was used instead of F-127 for Ti-E (P-123). [b] After calcination at 380 °C for 5h; A, anatase; R, rutile; B, brookite. [c] Calculated by applying the Scherrer formula on the anatase (101) or rutile (110) diffraction peak.

3. Results and Discussion

3.1. Effects of Solvent on the Synthesis of Titania. Table 1 shows the synthetic conditions for mesoporous titania materials. Pure anatase titania was obtained when methanol was used as the solvent (sample Ti-M). When ethanol or 1-butanol was used as solvent, bicrystalline titania (anatase and rutile) was obtained (Ti-E or Ti-B). To investigate the effects of cosolvent on the synthesis, 0.03 mol of DD water was introduced into the systems. Bicrystalline (anatase and rutile), tricrystalline (anatase, rutile and brookite), and pure rutile phase were formed in methanol (Ti-MH), ethanol (Ti-EH), and 1-butanol (Ti-BH) or 1-octanol (Ti-OH) systems, respectively. When 2 mL of concd hydrochloric acid was introduced as cosolvent to the ethanol system, pure rutile phase (Ti-HCl) was obtained instead of bicrystalline TiO_2 (Ti-E). Block copolymer P123 was also used in ethanol system and the same results were obtained. It is clear that by proper selection of solvent and cosolvent, the phase and phase composition in the case of a mixed phase can be readily controlled. And this makes the systematic investigation of the photocatalytic activity of titania materials feasible. It is noted here that TGA data confirmed that the surfactant F-127/P123 was completely removed after calcination at 380

(27) Zhang, H.; Banfield, J. F. *J. Mater. Chem.* **1998**, *8*, 2073. Zhang, H.; Banfield, J. F. *J. Phys. Chem. B* **2000**, *104*, 3481.
(28) Fotou, G. P.; Pratsinis, S. *Chem. Eng. Commun.* **1996**, *151*, 251.
(29) Abe, R.; Sayama, K.; Domen, K.; Arakawa, H. *Chem. Phys. Lett.* **2001**, *344*, 339.
(30) Yu, J. C.; Yu, J.; Ho, W.; Zhang, L. *Chem. Commun.* **2001**, 1942.

°C for 5 h. The phase content was calculated according to Zhang and Banfield[27] (see Section 3.2 for details).

The formation of anatase and rutile phases is related to the acidity during the synthesis.[31] The dissolution of $TiCl_4$ in alcohols ($C_mH_{2m+1}OH$) is exothermic and generates HCl gas and a collection of chloro-alkoxides $TiCl_{4-x}(OR)_x$ ($R = C_mH_{2m+1}$).[32] The resulting solution is acidic although the solubility of HCl in all of the alcohols used here is quite low as compared with that of water. The nondissolved HCl is released as gas in this process. With the increase of carbon number in the alcohol, the steric hindrance of the alkoxyl group to replace chlorine in the $TiCl_4$ becomes higher, thus more chlorine stays in the system. The next step is the formation of titania from the chloro-alkoxide species. In this step, water and HCl are produced. But this time, HCl is dissolved easily in water. Because more chlorine stays with the system after the first step as the number of carbon increases in the alcohol, the acidity of the system increases with the carbon number. When DD water was used as a cosolvent with alcohols, more HCl could dissolve in water, thus the acidity of the system could be higher than when water was not used. On the basis of the arguments above, it seems reasonable to suggest that low acidity favors the formation of anatase, whereas high acidity favors rutile. The formation mechanism of brookite phase is not well understood. However, hydrothermal treatment in the presence of a strong acid benefits its formation.[18,33]

Acidity is believed to determine the crystal structure. The dissolution of $TiCl_4$ in alcohols results in acidity of the system. By simply varying the solvent and cosolvent (methanol, ethanol, 1-butanol, or 1-octanol, with or without water), pure anatase, rutile, bicrystalline (anatase and rutile), and tricrystalline (anatase, rutile, and brookite) TiO_2 are successfully synthesized. If other titania precursors such as titanium alkoxide (titanium ethoxide, titanium isopropoxide, or titanium butoxide) are used instead of $TiCl_4$ under the same conditions, usually only anatase TiO_2 is obtained.

3.2. XRD, SEM, and TEM. All the materials in Table 1 were examined by XRD analysis. The XRD patterns of four of the samples were selected and are presented in Figure 1. All the diffraction peaks could be indexed as pure anatase TiO_2 (JCPDS, no. 21-1272) for sample Ti-M, rutile TiO_2 (JCPDS, no. 21-1276) for Ti-BH, bicrystalline (anatase and rutile) for Ti-E, and tricrysalline (anatase, rutile, and brookite) titania (brookite, JCPDS, no. 29-1360) for Ti-EH.

The phase contents of the samples were calculated from the relative peak intensities of anatase (101) and rutile (110) for bicrystalline anatase and rutile phases. For tricrystalline phases, the phase contents were calculated from the integrated intensities of anatase (101), rutile (110), and brookite (121) peaks with

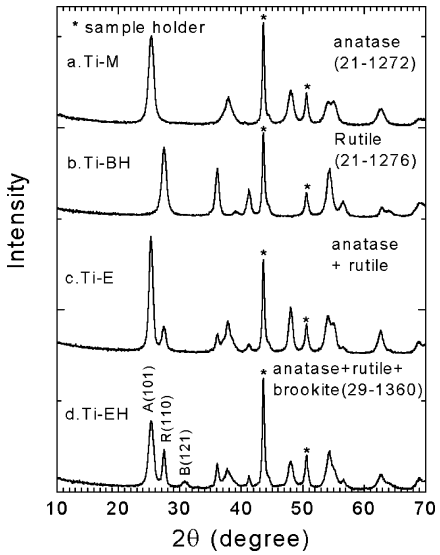

Figure 1. Wide angle XRD patterns of mesoporous TiO_2 after calcination at 380 °C for 5 h: (a) anatase (Ti-M), (b) rutile (Ti-BH), (c) bicrystalline (Ti-E), and (d) tricrystalline (Ti-EH).

the following formulas according to Zhang and Banfield[27]

$$W_A = k_A A_A/(k_A A_A + A_R + k_B A_B) \quad (1)$$

$$W_R = A_R/(k_A A_A + A_R + k_B A_B) \quad (2)$$

$$W_B = k_B A_B/(k_A A_A + A_R + k_B A_B) \quad (3)$$

In eqs 1, 2, and 3, W_A, W_R, and W_B represent the weight fractions of anatase, rutile, and brookite, respectively. A_A, A_R, and A_B are the integrated intensities of anatase (101), rutile (110), and brookite (121) peaks, respectively. The variables k_A and k_B are two coefficients. It was found that $k_A = 0.886$ and $k_B = 2.721$.[27]

XRD was used to investigate the phase stability and phase transformation. For pure anatase (Ti-M) and tricrystalline titania (Ti-EH), when calcined at 600 °C for 2 h, the crystal phases of anatase, rutile, and brookite were retained and no phase transformation occurred. However, the intensity of the peaks became stronger and well-resolved, indicating that larger particles were formed. When the calcination temperature was increased to 700 °C, anatase and rutile were retained, but brookite phase disappeared from the original tricrystalline phase due to the phase transformation of brookite to anatase. With a further increase in temperature, the phase transition of anatase to rutile began at 750 °C and the transition terminated at 900 °C after kept at that temperature for 2 h.

Low angle XRD patterns of the samples are presented in Figure 2. Low angle peak appeared in the as-synthesized sample (Ti-E), indicating the formation of mesostructure of titanium and polymer. After calcination at 380 °C for 5 h, the low angle peak shifted to lower diffraction angle (2θ) and the mesoscopic order was preserved in the sample of pure anatase phase (Ti-M) and bicrystalline phase (Ti-E), but disappeared or shifted to even lower angle beyond the X-ray diffractometer for pure rutile (Ti-BH) and tricrystalline phases (Ti-EH). Similar displacement to higher d spacing upon calcination was also observed in some alumina materi-

(31) Wang, C.; Deng, Z.-X.; Zhang, G.; Fan, S.; Li, Y. *Powder Technol.* **2002**, *125*, 39.
(32) Grosso, D.; Soler-Illia, G. J. de A. A.; Babonneau, F.; Sanchez, C.; Albouy, P.-A.; Brunet-Bruneau, A.; Balkenende, A. R. *Adv. Mater.* **2001**, *13*, 1085.
(33) Pottier, A.; Chanéac, C.; Tronc, E.; Mazerolles, L.; Jolivet, J.-P. *J. Mater. Chem.* **2001**, *11*, 1116.

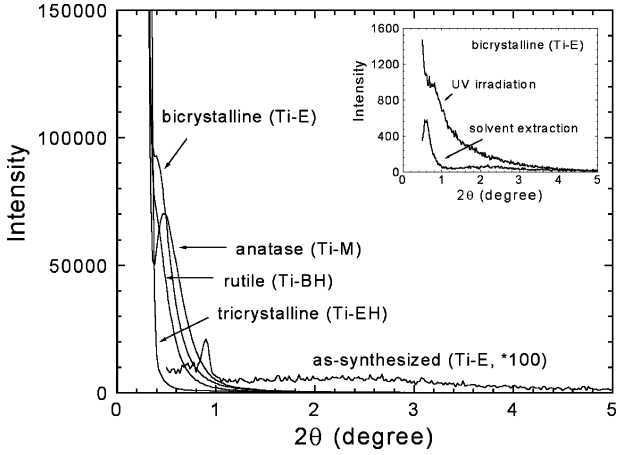

Figure 2. Low angle XRD patterns for as-synthesized sample (Ti-E), pure anatase (Ti-M), pure rutile (Ti-BH), bicrystalline (Ti-E), and tricrystalline TiO_2 (Ti-EH) after calcination at 380 °C for 5 h. Inset shows low angle XRD patterns for as-synthesized Ti-E by UV irradiation for one week, and solvent extraction using ethanol at 80 °C for 10 h.

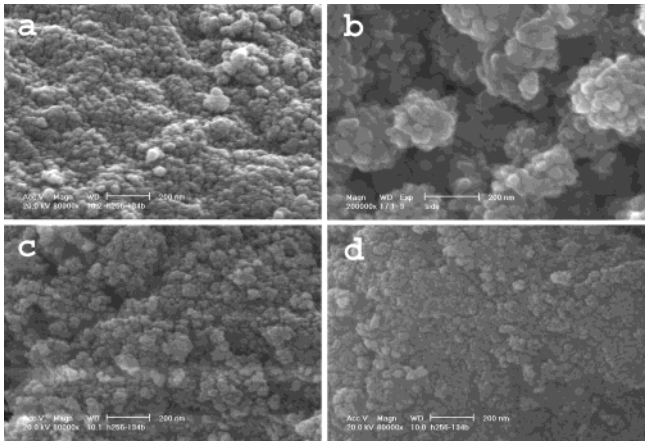

Figure 3. SEM images of mesoporous TiO_2 with (a) anatase (Ti-M), (b) rutile (Ti-BH), (c) bicrystalline anatase and rutile (Ti-E), and (d) tricrystalline frameworks (Ti-EH) after the sample calcination at 380 °C for 5 h.

als and mesoporous titania, probably due to the pore coalescence.[13] Only one XRD peak or no peaks in the low angle range indicate that no long-range order or disordered pore arrangement exists in our samples. To verify whether pore collapse is possible during the calcination, we also used UV irradiation for one week or solvent extraction using ethanol at 80 °C for 10 h for as-synthesized Ti-E sample. The low angle XRD patterns are shown in the inset of Figure 2. From TG/DTA analysis and N_2 adsorption/desorption measurement, the surfactant F-127 or P-123 cannot be removed completely by both methods. We also examined low-angle XRD for as-synthesized Ti-E at different temperature calcination; the low-angle peak existed at 100 and 200 °C calcination for 10 h, but disappeared after 300 °C calcination. Scanning electron microscopy (SEM) images (Figure 3) show the morphologies for mesoporous pure anatase (Ti-M), rutile (Ti-BH), bicrystalline (Ti-E), and tricrystalline TiO_2 (Ti-EH). The fine particulate morphology indicates that the mesoporosity is probably partly due to the intraparticle porosity, and partly due to the interparticle porosity.

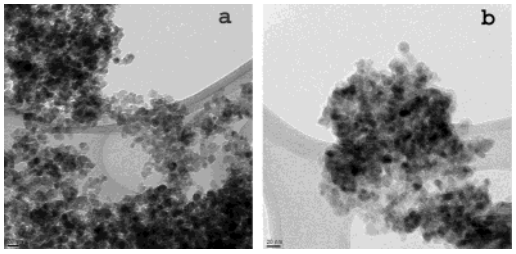

Figure 4. TEM images of mesoporous TiO_2 with (a) anatase (Ti-M), and (b) tricrystalline (Ti-EH) frameworks after the sample calcination at 380 °C for 5 h.

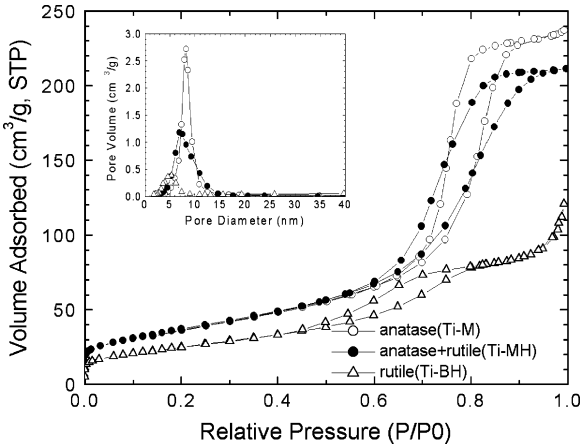

Figure 5. N_2 adsorption/desorption isotherm of the mesoporous TiO_2 with pure anatase (Ti-M), pure rutile (Ti-BH), and bicrystalline anatase and rutile (Ti-MH) frameworks after calcination at 380 °C for 5 h, the inset is the BJH pore size distribution plot.

TEM images of mesoporous TiO_2 with (a) anatase (Ti-M), and (b) tricrystalline (Ti-EH) frameworks, after the sample calcination at 380 °C for 5 h are presented in Figure 4. No mesostructure with long-range order can be observed in the TEM images. This is consistent with the low-angle XRD results, which shows the mesoporosity is mainly due to the interparticle porosity. The crystalline sizes estimated from the TEM images are in good agreement with that calculated from XRD pattern by using the Scherrer equation. The selected-area electron diffraction patterns confirm the crystalline anatase, or tricrystalline with anatase, rutile, and brookite, respectively.

3.2. N_2 Adsorption. Figures 5 and 6 show the N_2 adsorption/desorption isotherms of titania with pure anatase (Ti-M), pure rutile (Ti-BH), bicrystalline with anatase and rutile (Ti-MH) after calcination at 380 °C for 5 h, and tricrystalline (Ti-EH) after calcination at 380 and 500 °C for 5 h, respectively. Barrett−Joyner−Halenda (BJH) analysis of the desorption isotherms is shown in the inset. A clear hysteresis loop at high relative pressure is observed, which is related to the capillary condensation associated with large pore channels. The BET surface area, pore parameter, and pore volume of the mesoporous titania samples are summarized in Table 2 and compared with the results that have been reported by others. For the tricrystalline sample, the BET surface area is 391 m^2/g after it is calcined at 380 °C. This is the highest BET surface area among the calcined samples with crystalline framework. And in fact this value is comparable with that of the amorphous titania. The surface area decreased to 86

Table 2. XRD and N_2 Adsorption−Desorption Results for Mesoporous TiO_2

XRD (after calcination)	BET (m^2/g)	pore size (nm)	pore volume (cm^3/g)	ref.
P-TiO_2, amorphous	200 (350 °C)	3.2		2
P-TiO_2, amorphous	47−63 (250 °C)			3
P-TiO_2, amorphous	712 (200 °C)	2.4		4
TiO_2, amorphous	180 (300 °C)			7
TiO_2, amorphous	467 (350 °C)			8
anatase	79 (450 °C)			
TiO_2, amorphous	310 (300 °C)	3.6		12
TiO_2, semi-anatase	246 (300 °C)	2.98		11
TiO_2, semi-anatase	606 (350 °C)	3.5		13
TiO_2, semi-anatase	266−370 (350 °C)	2−2.5		14
TiO_2, semi-anatase	205 (400 °C)	6.5	0.22	15
TiO_2, semicrystalline	150−250 (350 °C)	4.1−6.3	0.2−0.4	20
TiO_2, anatase	201 (350 °C)	4.4	0.271	16
anatase + brookite	134 (500 °C)	8.0	0.336	
TiO_2, anatase	144 (400 °C)	3.7		18
anatase + brookite	128 (400 °C)	9.2	0.30	
TiO_2, anatase, brookite	235−310	3.5−4.4	0.24−0.32	22
TiO_2, anatase (Ti-M)	135 (380 °C)	8.2	0.36	this work
	56 (600 °C)	11.4	0.18	this work
rutile (Ti-BH)	91 (380 °C)	5	0.15	this work
bicrystalline (Ti-MH)	135 (380 °C)	7	0.33	this work
tricrystalline (Ti-EH)	391 (380 °C)	9.6	0.72	this work
	86 (500 °C)	11	0.30	this work
	51 (600 °C)	16	0.25	this work

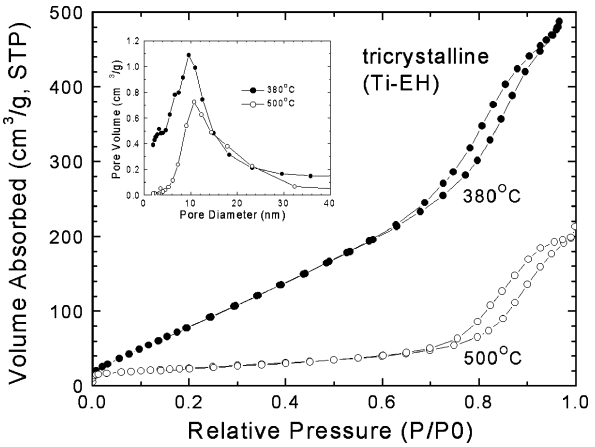

Figure 6. N_2 adsorption/desorption isotherm of the mesoporous TiO_2 with tricrystalline framework (Ti-EH) after calcination at 380 and 500 °C for 5 h, respectively, the inset is the BJH pore size distribution plot.

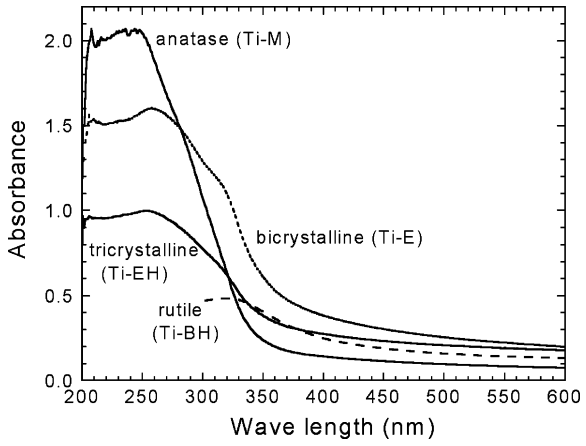

Figure 7. UV−visible absorbance spectra for mesoporous TiO_2 with pure anatase (Ti-M), rutile (Ti-BH), bicrystalline (Ti-E), and tricrystalline (Ti-EH) frameworks.

m^2/g after calcination at 500 °C. The average pore size increased from 9.6 to 11 nm. The pore diameter of 11 nm is the largest reported for mesoporous titania. The mesoporous tricrystalline titania retained its structural integrity and mesoporosity till calcination at 600 °C, where its BET surface area decreased to 51 m^2/g, pore volume decreased to 0.25 cm^3/g, and pore diameter increased to 16 nm.

Compared with the mesoporous titania with pure anatase or bicrystalline (anatase and rutile) phase, pure rutile has lower surface area, smaller pore diameter, and lower pore volume. A close examination of the XRD patterns for the mesoporous titania with different crystalline phases reveals that the reflections assigned to anatase are always broader than those for rutile, which implies larger mean particle sizes of rutile. And this probably is responsible for lower surface area of the rutile phase.

3.3. UV−visible Absorbance. Figure 7 shows the UV−visible absorbance (α) spectra for the mesoporous titania with pure anatase (Ti-M), pure rutile (Ti-BH), bicrystalline (Ti-E), and tricrystalline (Ti-EH) frameworks. For pure anatase, the significant increase in the absorption at wavelengths (λ) shorter than 380 nm can be assigned to the intrinsic band gap absorption of anatase. The band gap (E_g) is estimated to be 3.35 eV from the plot of $\alpha^{1/2}$ versus photon energy ($h\nu$). This value is slightly higher than the reported value for anatase (3.2−3.3 eV).[34] The band gap is a strong function of titania particle size for diameters less than 10 nm because of the well-known quantum size effect.[4] Thus, the higher band gap could be a result of small particle size (Table 1). The absorption spectrum of mesoporous rutile shows a lower absorption, and the calculated band gap is around 2.8 eV. This value is lower than the reported rutile (3.0−3.1 eV) and the reason is not clear.[34] For bicrystalline and tricrystalline titania, band gaps of 3.0 and 3.05 eV were determined, respectively. The band gap of brookite is 3.4 eV,[35] which is

(34) Linsebigler, A. L.; Lu, G.; Yates, J. T., Jr. *Chem. Rev.* **1995**, *95*, 735.
(35) Koelsch, M.; Cassaignon, S.; Guillemoles, J. F.; Jolivet, J. P. *Thin Solid Films* **2002**, *403−404*, 312.

higher than that of anatase and rutile, and this can explain the fact that the band gap of tricrystalline containing brookite is slightly larger than that of bicrystalline with anatase and rutile.

4. Conclusions

Using triblock copolymer as structure-directing agent and $TiCl_4$ as precursor, by simply varying the solvents, mesoporous titania with pure anatase, pure rutile, bicrystalline (anatase and rutile) with controlled phase composition, and tricrystalline (anatase, rutile, and brookite) frameworks have been successfully synthesized. The crystalline mesoporous titania are thermally stable and have high surface area and large pore diameter.

Acknowledgment. We acknowledge the financial support from Riverside Public Utilities, California Energy Commission, Pacific Fuel Cell Corporation, and UC-MART.

CM0302882